Supporting information to 'Plasma Enhanced Atomic Layer Deposition of Nickel and Cobalt Phosphate for Lithium Ion Batteries'

Lowie Henderick,† Ruben Blomme,† Matthias Minjauw,† Jonas Keukelier,† Johan Meersschaut,‡ Jolien Dendooven,† Philippe Vereecken,‡ and Christophe Detavernier*,†

†*Department of Solid State Sciences, Ghent University, Krijgslaan 281 S1, 9000 Gent, Belgium*

‡*imec, Kapeldreef 75, B-3001 Heverlee, Belgium*

E-mail: Christophe.Detavernier@Ugent.be

Deposition of nickel phosphate

To complete the thin film characterisation, the surface morphology before and after an anneal into a crystalline phase was studied using SEM (figure S1(a,b,c)). The as-deposited, amorphous, layer showed to be a closed and relatively smooth film. The crystallisation into $Ni_3(PO_4)_2$ clearly increased the roughness of the layer, with the material agglomerating into irregularly shapes islands. This is also observed after crystallisation into Ni_2P, although the agglomerates are more spherical, smaller and more densely packed. The same conclusion can be drawn from AFM measurements, as can be seen in figure S1(d,e,f). The roughness clearly increased after annealing, going from a root mean square of 1.6 nm to 4.6 nm with the crystallisation into $Ni_3(PO_4)_2$ and 7.2 nm after crystallisation into Ni_2P.

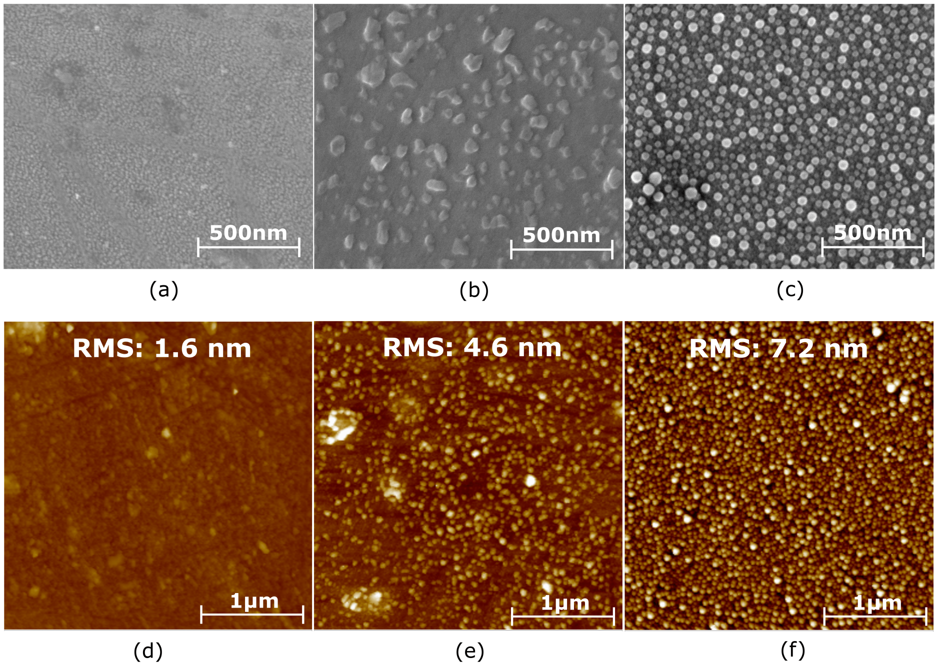

Figure S1: SEM and AFM images of the (a,d) as-deposited nickel phosphate, (b,e) after crystallisation into $Ni_3(PO_4)_2$ and (c,f) after crystallisation into Ni_2P. The root mean square of each AFM measurement is also presented, and the same color scale has been used for the three different samples.

The XRD diffraction pattern of nickel phosphate resulting from a TMP* - O_2* - $NiCp_2$ - O_2* process before and after anneal was also measured and is shown in figure S2. Two peaks (highlighted by the black arrows) are observed in the as deposited diffraction pattern, indicating that (to some degree) crystalline $Ni_3(PO_4)_2$ might have been formed during deposition. Only an anneal in helium and oxygen atmosphere was attempted, as the main goal was to see if the nickel could be further oxidised during the anneal. However, no clear changes were observed during the anneal in oxygen atmosphere while additional $Ni_3(PO_4)_2$ peaks are present after anneal in helium.

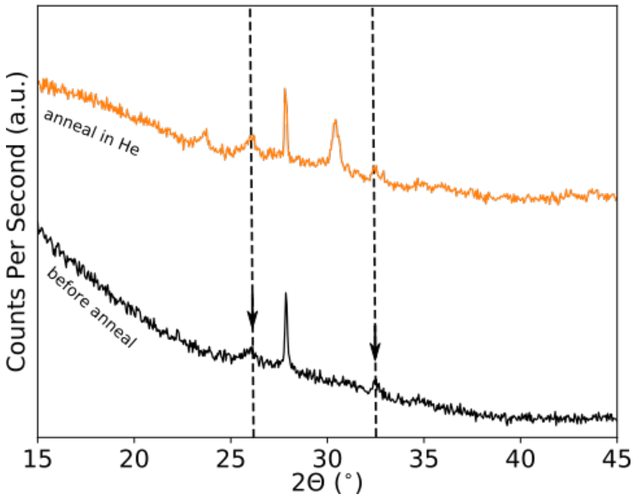

Figure S2: XRD diffraction pattern of as deposited nickel phosphate from the TMP* - O_2* - $NiCp_2$ - O_2* process, compared to the diffraction pattern after anneal in helium and oxygen. The black arrows denote peaks that can indicate a degree of crystallisation during the PE-ALD process.

PE-ALD phosphates as LIB electrodes

Reaction mechanism. To study the nature of the electrochemical activation of nickel phosphate, the observed charge of the activation peak can be compared to the expected charge for a particular reaction (similar to what was done for PE-ALD iron phosphate in the work of Dobbelaere et al.). The latter can be calculated using Faraday's law:

$$\frac{Q}{A} = \frac{nde\rho N_A}{M}$$

with $\frac{Q}{A}$ the charge per surface area, e the elementary charge, N_A is Avogadro's constant, n is the number of electrons transferred in the redox reaction, ρ is the density of the film, d is the thickness of the film and M is the molar mass. From the ERD composition, the molar mass of one $NiP_{0.5}O_2$ unit (normalised on nickel, to calculate the amount of electrons transferred per nickel atom) is 107 g/mol. The thickness and density (measured by XRR) were respectively 28 nm and 3.5 g/cm^3. This results in $\frac{Q}{A} = 2.4 * n$ μAh/cm^2, with the measured charge of the activation peak being equal to approximately 5.7 μAh/cm^2. A total of approximately 2.4 electrons (or lithium ions) per nickel atom have thus been transferred during activation. This seems to point towards a conversion reaction from Ni^{2+} to Ni^0 (a total of 2 electrons exchanged, with an expected charge of 4.8 μAh/cm^2), but with an excess charge (the remaining 0.9 μAh/cm^2 that was unaccounted for with respect to the measured charge) that can be attributed to the formation of a solid electrolyte interface (SEI).
The peak in the following anodic scan shows a capacity of 4.1 μAh/cm^2, or a total of 1.7 electrons (or lithium ions) transferred per nickel atom. This could be in line with the reversible conversion reaction (Ni^{2+}/Ni^0) of the nickel phosphate, or alternatively with a (de-)alloying process that involves the exchange of approximately 1.7 lithium ions per nickel atom. A coulombic efficiency close to 100% was then observed in the following cycles, indicating a reversible charge/discharge redox couple.

For the analysis of cobalt phosphate, a reliable compositional ERD analysis of the deposited layer would be needed. As this was not done in this work, only an assumption on the reaction mechanism can be made. Assuming a stoichiometry of $CoP_{2.3}O_{6.7}$, the molar mass of one unit would be 237 g/mol. The film thickness and density are 28 nm and approximately 3.2

g/cm^3 (measured with XRR). This results in $\frac{Q}{A} = 1 * n$ μAh/cm^2. An activation in which Co^{2+} is thus reduced to metallic cobalt would result in a charge of 2 μAh/cm^2. The measured charge during the activation of this cobalt phosphate is 4.1 μAh/cm^2. This could again be in line with the conversion reaction, with the formation of an SEI layer resulting in excess charge. In the following anodic scan, a charge of 2.1 μAh/cm^2 is observed. This would also agree with 2 electrons being transferred per cobalt atom, indicating a similar reaction path as for the nickel phosphate.

Cyclic voltammetry of nickel phosphate. For completion of the cyclic voltammetry study of the PE-ALD nickel phosphate, the comparison between layers deposited with the TMP* - O_2* - $NiCp_2$ - O_2* process and the TMP* - O_2* - $NiCp_2$ process is presented in figure S3. Here it is observed that the shape of the voltammograms is very similar, meaning the additional oxygen plasma did not dramatically change the electrochemical nature of the phosphate.

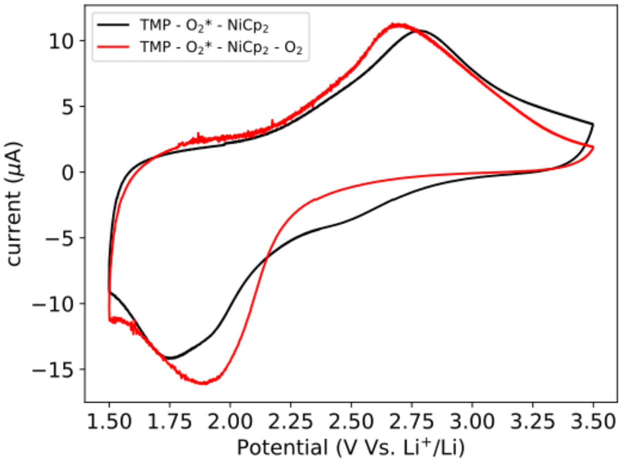

Figure S3: Cyclic voltammogram of nickel phosphate deposited with and without an additional oxygen plasma. The voltammogram is recorded after the electrochemical activation at low potential, and is measured at a scan rate of 1 mv/s.

In addition, the activation of PE-ALD nickel phosphate (without additional oxygen plasma) is also presented, together with several subsequent cycles, in figure S4. Here, the shift of the cathodic peak after activation is clearly visible, as well as the disappearance of the high voltage component of the cathodic peak throughout cycling.

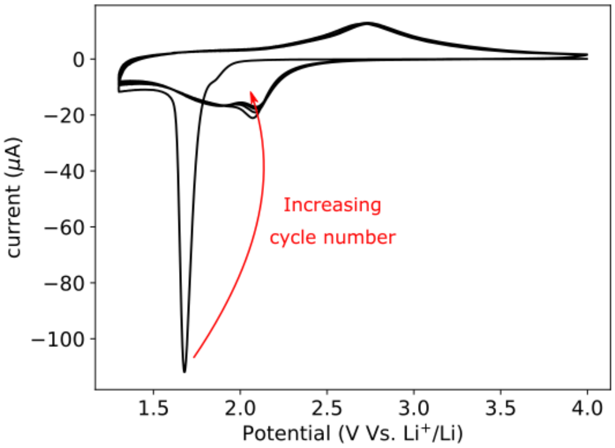

Figure S4: Initial cycles of nickel phosphate, with the red arrow denoting how the cycle number evolves. The voltammogram is measured at a scan rate of 1 mv/s.